

Elastic electron scattering from CF₃I

Jessica R. Francis-Staite, Brett A. Schmerl, and Michael J. Brunger

ARC Centre for Antimatter-Matter Studies, School of Chemical and Physical Sciences, Flinders University, GPO Box 2100, Adelaide, SA 5001, Australia

H. Kato

Department of Physics, Sophia University, Chiyoda-ku, Tokyo 102-8554, Japan

Stephen J. Buckman

ARC Centre for Antimatter-Matter Studies, Research School of Physical Sciences and Engineering, Australian National University, Canberra, ACT 0200, Australia

(Received 8 December 2009; published 8 February 2010)

Experimental results are reported for elastic differential and integral cross sections for electrons scattering from CF₃I. These measurements were made at ten incident electron energies in the range 10–50 eV, with a scattered electron angular range of 20°–135°. Where possible, comparison is made to the only other comprehensive experimental set of results available in the literature [M. Kitajima *et al.*, J. Phys. B **35**, 3257 (2002)] and to calculated cross sections from the Schwinger multichannel with pseudopotentials method [M. H. Bettega *et al.*, J. Phys. B **36**, 1263 (2003)]. In general, quite good agreement is found between the present results and those of the earlier studies.

DOI: [10.1103/PhysRevA.81.022704](https://doi.org/10.1103/PhysRevA.81.022704)

PACS number(s): 34.80.Bm

I. INTRODUCTION

Semiconductor plasma etch technology traditionally employs feedstock gases such as CF₄, C₂F₆, C₃F₈, CHF₃ and *c*-C₄F₈. All these molecules have large global warming potentials because they absorb radiation in the infrared window (800–1300 cm⁻¹), and all are thought to persist in the Earth's atmosphere for extended periods [1]. Because the current generation of plasma reactors still release a large proportion of feedstock gas into the atmosphere, one way of reducing these harmful emissions is to utilize different etchant gases whose properties lessen climate change effects. In particular, trifluoroiodomethane (CF₃I) has attracted some interest in this regard. The specific properties that make this species viable as an alternative feedstock gas include its short atmospheric lifetime (<2 days) due to UV photolysis [2] and that the photolysis products are water-soluble compounds which are short-lived in the atmosphere due to the 10-day hydrological cycle [3]. In addition, due to the relatively weak C–I bond, it is possible, within a plasma reactor, to dissociate CF₃I by direct electron impact [4,5]. This leads to the production of high yields of CF₃ radicals, as well as CF₂ and CF radicals, which play crucial roles in the etching process. Thus, CF₃I represents, for the reasons outlined above, a real alternative to the traditional plasma reactor feedstock gases.

Because the large-scale computer models that have been developed for plasma processing require reliable and accurate electron scattering cross sections to simulate conditions within a plasma processing cell [6], it is somewhat surprising to find how little of such data are actually available in the literature [3]. An excellent recent summary and critical evaluation of *e*⁻ + CF₃I cross sections is given by Rozum *et al.* [3], who drew heavily from the data compilation of Christophorou and Olthoff [7]. Other relevant work includes the total-cross-section measurements from Kawada *et al.* [8] and corresponding complex optical method calculations from

Joshipura *et al.* [9], experimental elastic differential cross sections (DCSs) from Kitajima *et al.* [10] and the theoretical elastic DCSs, integral cross sections (ICSs), and momentum transfer cross sections from Bettega *et al.* [11]. These last two studies are the most relevant in terms of the current work, and we compare the present results to them later in this paper. We note that while Kitajima *et al.* [10] reported an extensive range of DCS measurements between 1.5 and 60 eV, at higher incident energies they did so at only 10, 20, and 60 eV. Hence, part of the rationale for this study was to increase our knowledge for the elastic scattering process between 10 and 60 eV. In addition, Kitajima *et al.* [10] did not report elastic ICSs. Currently the ICSs are probably most relevant to the plasma modeling community; this work was also undertaken to provide such data and to enable a comparison to be made with the results from the Schwinger multichannel (SMC) computations of Bettega *et al.* [11]. Finally, for completeness, we note the CF₃I ionization cross-section measurements from Jiao *et al.* [12] and Onthong *et al.* [13] and the theoretical ionization cross sections from Joshipura *et al.* [14]. A further rationale for the present measurements stems from the fact that we are presently engaged in a series of experiments involving electron collisions with molecular radicals [15]. A target of interest is the CF₃ radical, which can be efficiently produced through pyrolysis of a beam of CF₃I molecules. The resulting beam contains a number of daughter fragments, including CF₃ and I, and some of the parent molecule, CF₃I. In order to effectively estimate elastic scattering cross sections for CF₃, we also need to understand the elastic DCS for the remaining beam constituents. Thus, the present measurements also provide the required data for the CF₃I parent molecule.

In the next section of this paper, we describe the apparatus and techniques employed in the measurements. Thereafter, in Sec. III, results and a discussion of those results are presented.

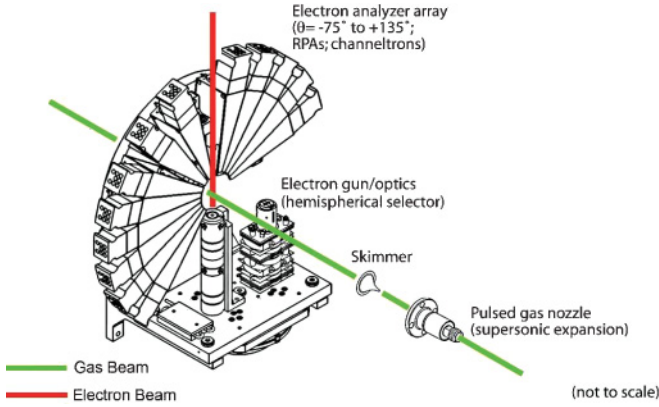


FIG. 1. (Color online) Schematic diagram of the present apparatus (see text for further details).

Finally, in Sec. IV we draw some conclusions from the present investigation.

II. EXPERIMENTAL DETAILS AND MEASUREMENT TECHNIQUES

The CF_3I elastic DCSs were measured using a crossed beam apparatus (see Fig. 1) that has been described in detail previously [16], but in the interests of completeness a brief description is also included here. This apparatus consists of three main vacuum chambers and a differentially pumped subchamber. The first chamber houses a supersonic nozzle (Parker Hannifin, General Valve Division, Series 9 pulsed valve) with a diameter of 0.8 mm; the nozzle was pulsed at 10 Hz. This chamber was pumped by a 10-in. diffusion pump (Varian VSH10). A 1-mm-diam skimmer mounted 8 cm from the pulsed nozzle separated the first and second chambers and served to collimate the molecular gas jet.

The second chamber contained an analyzer array of 13 wedges mounted radially around the interaction region. Each wedge contained a Channeltron (Sjuts KBL210) mounted behind a retarding potential analyzer, which provided an energy resolution of approximately 1.3 eV [16]. For the present study, ten of these analyzers were used and data were recorded for the following angles: -45° , -30° , 20° , 40° , 60° , 75° , 90° , 105° , 120° , and 135° . This chamber was pumped on by a turbomolecular pump (Pfeiffer TPU 261C). We note that the second chamber also housed a subchamber that contained an electron monochromator [16], which was evacuated using a second turbomolecular pump (Pfeiffer TPU071P). For the purposes of this study, the electron monochromator energy ranged from 10 to 50 eV. A Faraday cup measured the electron monochromator current, which varied between 6 and 12 nA over the energy range used. The final chamber was pumped by a 6-in. diffusion pump (Varian VHS6) and contained a Wiley-McLaren time-of-flight mass spectrometer. This device was used to analyze the constituents of the beam formed by pyrolysis but, because this analysis was not used in this investigation, no further details are given here.

Labview version 8.2, in conjunction with a custom-built timing controller, a pulsed nozzle driver, and various power supplies, was used to control each experiment and to record

the data. Four National Instruments counter-timer cards, used in conjunction with four BNC-2121 devices, allowed for data to be collected simultaneously at all the scattering angles. Labview's ability to set timing windows, and the pulsed nature of the experiment, also allowed for both background scattering and signal plus background scattering to be recorded in the same run, thereby facilitating shorter experimental run times.

The present DCSs were set to an absolute scale using the pulsed supersonic relative density method (p-SSRDM), a method that has also been reported in detail in a previous paper [17]. Briefly, this method determines the absolute cross section of a target gas, in this case CF_3I , by comparing the amount of elastic scattering from the target gas to that from a reference gas, in this case CF_4 . The p-SSRDM can be applied when each gas beam is collimated in the region of free molecular flow, so that the spatial distribution of both reference and target gases can be made identical, thereby allowing the centerline intensity of each gas beam to be determined. In our case we matched the spatial distribution of the gases by using a polyatomic reference gas with the same stagnation pressure as our target (400 mbar). The centerline intensity ratio $\frac{I_T}{I_R}$ was determined using the relationship shown in Eq. (1) [18]:

$$\frac{I_T}{I_R} = \frac{P_R Q_T v_{\infty T} S_R}{P_T Q_R v_{\infty R} S_T}, \quad (1)$$

where the subscripts T and R denote the target and reference, respectively; P is the difference in chamber pressure from the “gas on” to “gas off” condition and is measured directly using a full-range vacuum gauge (Pfeiffer PTR26000), while Q is the electron impact ionization cross section at the cold cathode filament voltage of 150 V. In the present study we use the theoretical values of Antony *et al.* of 8.58 and 5.71 \AA^2 for CF_4 and CF_3I , respectively [19]. Together, the measured change in pressure and the ionization cross section at 150 eV enable the absolute change in pressure for each gas to be determined. In Eq. (1) we also note that v_{∞} is the terminal velocity and S is the pumping speed. The terminal velocity is calculated as

$$v_{\infty} = \sqrt{\frac{2k_B T_0}{m} \left(\frac{\gamma}{\gamma - 1} \right)}, \quad (2)$$

where k_B is Boltzmann's constant, T_0 is the temperature behind the expansion nozzle, m is the atomic weight of the molecule, and γ is the adiabatic constant. The adiabatic constant is further defined as

$$\gamma = \frac{f + 2}{f}, \quad (3)$$

where f is the sum of the number of degrees of rotational, vibrational, and translational freedom of the molecule. For CF_4 , γ was determined to be $\frac{9}{7}$, while γ for CF_3I was $\frac{7}{6}$.

Our current method differs from that of Maddern *et al.* [17]; we no longer calculate the pumping speed S based on the mass of the particle and the types of pumps utilized by our system, because these calculations were determined to only be accurate to within 30%. Instead we directly measure the pumping speed by logging the decrease in chamber pressure as a function of time and then using the relationship shown in Eq. (4):

$$P(t) = P(0) \exp -t \frac{S}{V}, \quad (4)$$

TABLE I. Experimental elastic differential cross sections of CF₃I for electron impact energies from 10 to 25 eV, in units of 10⁻¹⁶ cm² sr⁻¹.

Scattering angle (degrees)	Electron impact energy				
	10 eV	12 eV	15 eV	20 eV	25 eV
20					
30	61.92 ± 36.95	35.38 ± 12.92	14.67 ± 3.81	10.35 ± 3.97	32.50 ± 9.85
40	16.59 ± 4.57	11.68 ± 3.24	7.51 ± 1.92	3.13 ± 0.99	2.54 ± 0.76
45	9.64 ± 2.73	9.08 ± 3.26	3.89 ± 1.06	1.24 ± 0.72	2.47 ± 0.85
60	2.51 ± 0.69	1.32 ± 0.34	1.39 ± 0.38	1.19 ± 0.48	1.70 ± 0.58
75	1.90 ± 0.48	1.65 ± 0.41	1.84 ± 0.47	1.04 ± 0.28	0.49 ± 0.15
90	3.87 ± 0.98	2.25 ± 0.57	1.68 ± 0.43	0.61 ± 0.16	0.70 ± 0.21
105	3.85 ± 1.09	1.46 ± 0.62	1.19 ± 0.31	0.65 ± 0.18	0.47 ± 0.14
120	3.64 ± 1.38	0.86 ± 0.35	1.01 ± 0.27	0.70 ± 0.22	0.74 ± 0.23
135	11.27 ± 6.28	1.97 ± 0.84	1.67 ± 0.47	2.07 ± 1.27	1.34 ± 0.42

where $P(0)$ is the initial pressure, $P(t)$ is the chamber pressure as it changes with time, V is the chamber volume, and S , as defined earlier, is the pumping speed. Hence, we were able to more accurately find the ratio of the pumping speeds for the target and reference gases by determining the ratio of the linear trend lines for each gas. These linear trend lines were determined using plots of $\ln(P)$ versus time (s).

Once all the terms from Eq. (1) are known, the DCS is calculated using the relationship shown in Eq. (5):

$$\sigma_T = \frac{\dot{N}_T^e P_R Q_T v_{\infty T} S_R}{\dot{N}_R^e P_T Q_R v_{\infty R} S_T} \sigma_R, \quad (5)$$

where σ is the elastic DCS, \dot{N}^e is the number of true elastic counts recorded for each gas, and all other terms are as in Eq. (1).

The uncertainties for the measured DCSs were typically of the order of 30%, including an uncertainty on the reference DCS ($\sim 20\%$ [20]), the uncertainty for our measurement of the change in pressures ($\sim 5\%$), the uncertainty in the pumping speed calibration ($\sim 5\%$), the uncertainty in matching the spatial distribution of both reference and target gases ($\sim 10\%$), and as well the statistical variation in the elastically scattered signal for each angle and each energy for the target and reference gases. The uncertainties for our ICSs are estimated to

be typically $\sim 40\%$, which includes an additional uncertainty due to the DCS extrapolation procedure (to 0° and 180°) we employed (see later).

III. RESULTS AND DISCUSSION

In Tables I and II and Figs. 2–4, we report the present elastic DCSs for electron scattering from CF₃I. Also shown in Figs. 2–4 are the SMC results of Bettega *et al.* [11] and, at 10 and 20 eV, the previous DCS results from Kitajima *et al.* [10]. There are several general trends in the present data, which we now consider. First, all the DCSs suggest a marked increase in the magnitude of the cross section as the scattering angle is decreased. This observation is consistent with CF₃I having both a significant permanent dipole moment (1.05 D [11]) and average dipole polarizability ($\alpha = 58.72$ a.u. [11], or 52.42 a.u. [21]). Hence, this suggests that both of this target's properties play an important role in the scattering dynamics of this system. It is also clear from Figs. 2–4 that the shapes of the present DCSs are in very good accord with those of the SMC calculation and the corresponding data of Kitajima *et al.* at all energies where a direct comparison is possible.

With respect to the magnitudes of the DCSs, the present data are also in very good agreement with the SMC results

TABLE II. Experimental elastic differential cross sections of CF₃I for electron impact energies from 30 to 50 eV, in units of 10⁻¹⁶ cm² sr⁻¹.

Scattering angle (degrees)	Electron impact energy				
	30 eV	35 eV	40 eV	45 eV	50 eV
20					
30	3.79 ± 1.06	13.57 ± 4.41	2.84 ± 0.79	1.34 ± 0.47	1.23 ± 0.34
40	0.98 ± 0.29	1.59 ± 0.55	3.33 ± 1.01	0.88 ± 0.28	0.67 ± 0.19
45					0.36 ± 0.22
60	0.64 ± 0.17	0.89 ± 0.27	0.67 ± 0.18	0.63 ± 0.19	0.39 ± 0.10
75	0.36 ± 0.09	0.90 ± 0.27	0.72 ± 0.19	0.35 ± 0.11	0.25 ± 0.07
90	0.36 ± 0.09	0.29 ± 0.09	0.26 ± 0.07	0.14 ± 0.04	0.13 ± 0.03
105	0.19 ± 0.09	0.29 ± 0.10	0.46 ± 0.13	0.50 ± 0.21	0.28 ± 0.12
120	0.43 ± 0.12	0.66 ± 0.20	0.68 ± 0.19	0.71 ± 0.21	0.45 ± 0.12
135	0.61 ± 0.18	0.82 ± 0.25	0.73 ± 0.19	0.67 ± 0.20	1.06 ± 0.28

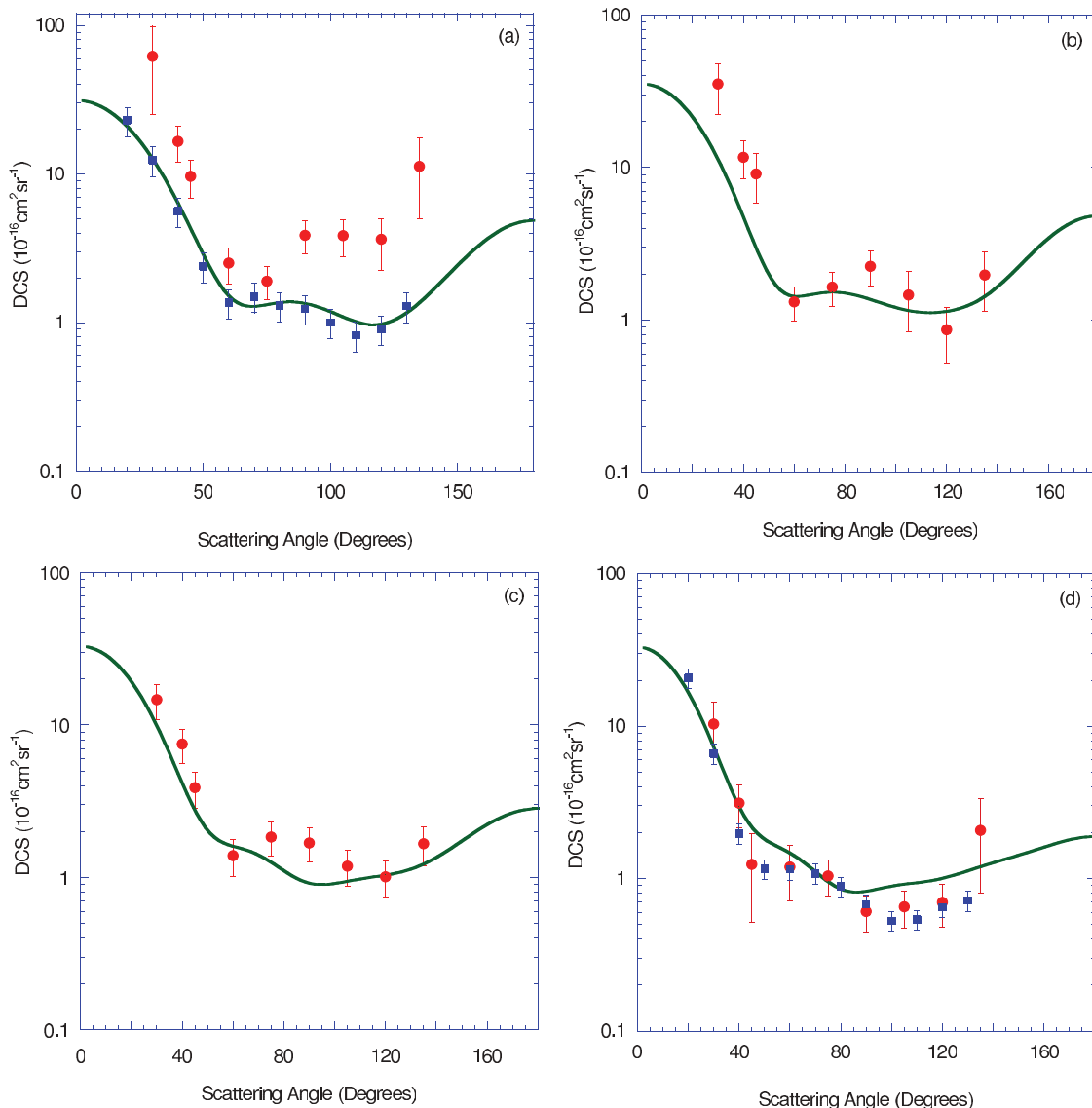


FIG. 2. (Color online) Elastic differential cross sections ($10^{-16} \text{ cm}^2 \text{ sr}^{-1}$) for electron impact on CF_3I from SMC calculations by Bettega *et al.* [11] (solid line), measurements of Kitajima *et al.* [10] (■), and the current measurements (●), for electrons of energy (a) 10, (b) 12, (c) 15, and (d) 20 eV.

(see Figs. 2–4), except at the lowest incident electron energy of this investigation (10 eV). This is particularly true when one also allows for the fact that the correction due to the long-range dipole interaction was not made by Bettega *et al.* Such a correction would have the effect of increasing the magnitudes of the DCSs at the smaller (more forward) scattered electron angles. If we now consider Fig. 5, for the elastic ICSs, we see that the SMC predicts two shape resonances in the 5–50 eV energy range. The first, with a peak in the ICS at around 7 eV, is quite strong and relatively narrow, while the second, with a peak in the ICS at ~ 12 eV, is relatively weaker and a little broader. The SMC calculation of Bettega *et al.* was performed within a static exchange approximation and a fixed-nuclei framework. It is well known that, when both polarization [22] and nuclear dynamics [23] are accounted for, the positions of any resonances typically move to lower

incident electron energies. It is therefore likely that the second resonance predicted by the SMC should physically occur at a lower energy (e.g., ~ 10 eV) than is currently the case. This may explain, at least in part, the apparent mismatch in the absolute values of the present 10-eV DCSs and those from the SMC computation. Certainly the angular structure observed in our 10-eV DCS is consistent with resonant decay into the elastic channel around this energy.

At 20 eV (see Fig. 2), the present DCS is found to be in very good agreement with that of Kitajima *et al.* over the common angular range of measurement. Although we do not specifically show it, we performed an interpolation (cross section versus energy at each scattered electron angle) between all the DCS data from Kitajima *et al.* and then compared those interpolated values against the present measured data. At all energies greater than and including 15 eV, very good

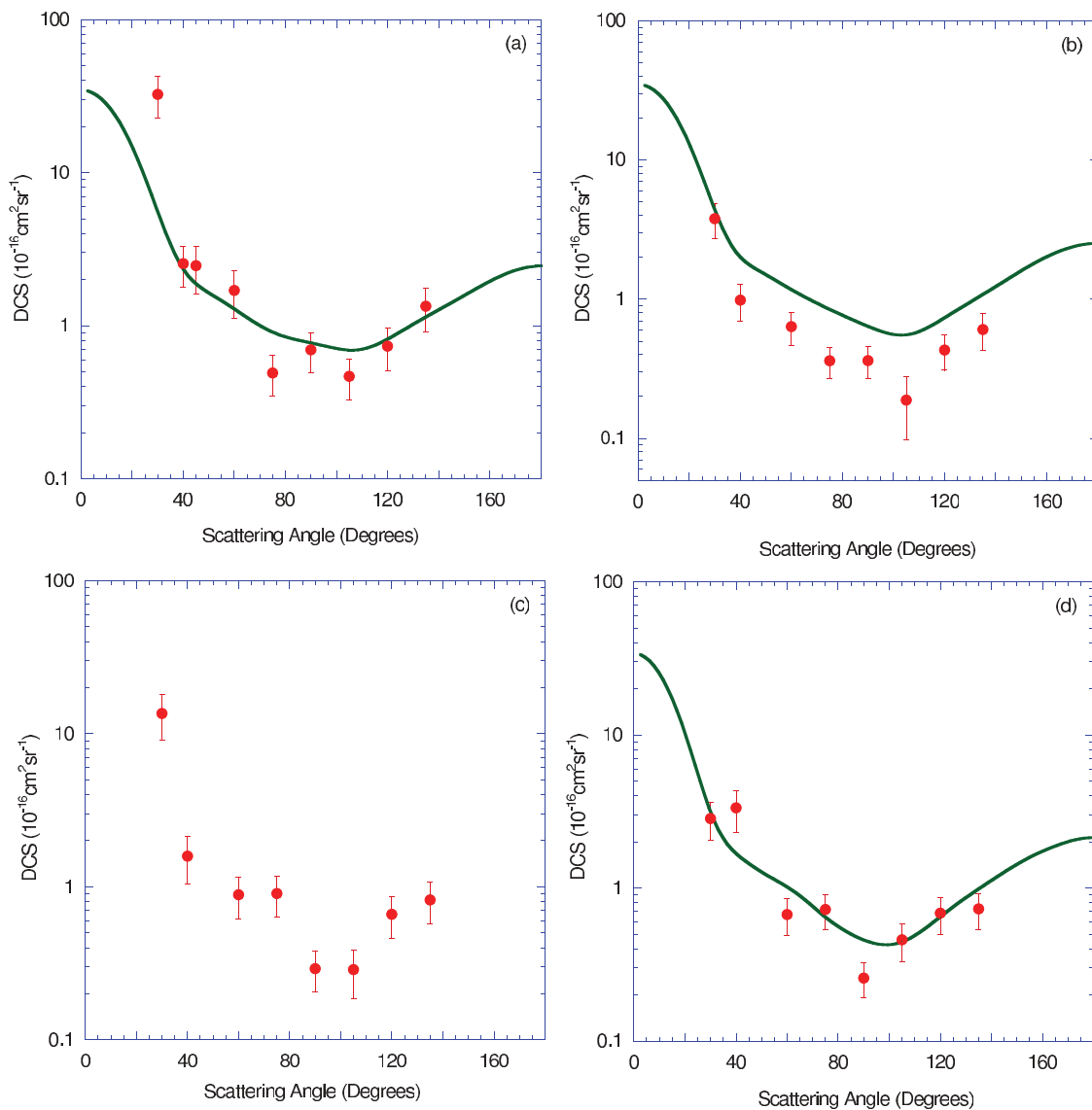


FIG. 3. (Color online) Elastic differential cross sections ($10^{-16} \text{ cm}^2 \text{ sr}^{-1}$) for electron impact on CF₃I from SMC calculations by Bettiga *et al.* [11] (solid line) and the current measurements (\bullet), for electrons of energy (a) 25, (b) 30, (c) 35, and (d) 40 eV.

agreement was found between the magnitudes and shapes of the present measured DCSs and those interpolated from the data of Kitajima *et al.* Of course, such an interpolation process would be inherently flawed if resonance effects were important in the collision dynamics; however, at energies greater than 15 eV, it appears resonant decay into the elastic channel is not a significant issue. This latter assertion is supported by both the SMC ICS calculated (see Fig. 5) results and the fact that our measured data and the interpolated results from Kitajima *et al.* [10] are in such good accord. At 10 eV (see Fig. 2) there is, however, a worrying discrepancy in magnitude between the current DCSs and those from Kitajima *et al.* While it is possible that some of the DCS magnitude discrepancy at 10 eV between our study and that of Kitajima and colleagues may be due to a small mismatch in the true energies of the respective measurements, this could not possibly explain all the observed disagreement here. We therefore undertook a detailed study

on the sensitivity of our 10-eV DCSs to the conditions under which they were measured. In all cases, including when we varied the target stagnation pressures, the p-SSRDM results were robust and entirely consistent with the values reported in Table I. As a consequence, we believe the apparent discrepancy in CF₃I at 10 eV can only be resolved by an independent measurement being undertaken.

Finally, in Fig. 5 and Table III, we report the present elastic ICSs for electron scattering from CF₃I. The present ICSs were derived, at each incident electron energy, by using our molecular-phase-shift analysis (MPSA) [24] approach to extrapolate the measured DCS to 0° and 180° and then perform the usual integration. An alternative extrapolation, where we employed the SMC theory to guide us, was also tried and the ICSs derived from these two procedures were consistent to within the $\sim 40\%$ uncertainty we conservatively cite as the error for these data. Note that it is the MPSA results that are

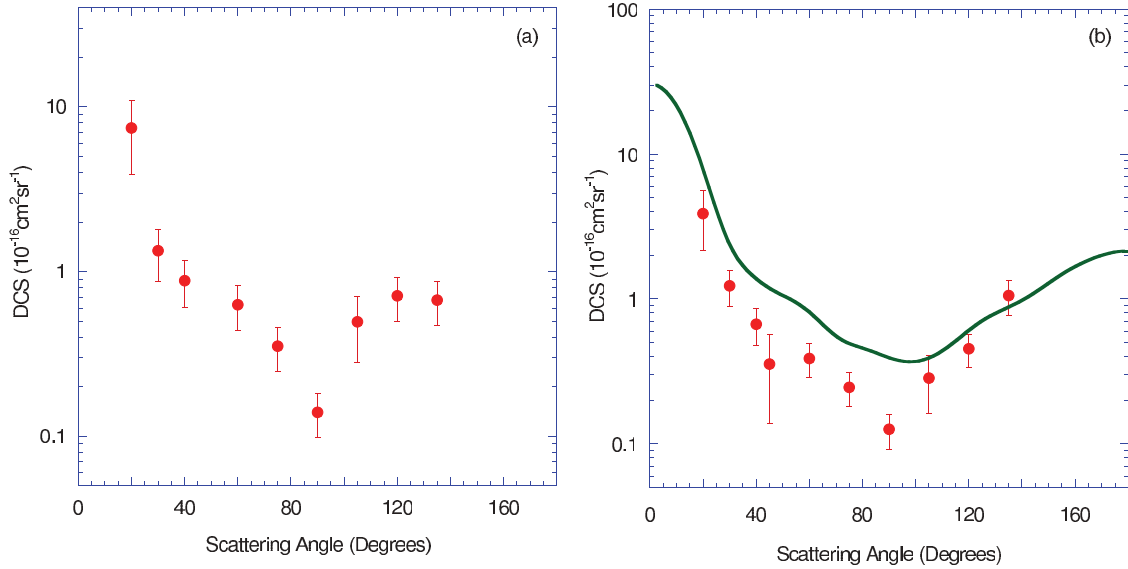


FIG. 4. (Color online) Elastic differential cross sections ($10^{-16} \text{ cm}^2 \text{ sr}^{-1}$) for electron impact on CF_3I from SMC calculations by Bettega *et al.* [11] (solid line) and the current measurements (\bullet), for electrons of energy (a) 45 and (b) 50 eV.

provided in Table III. In Fig. 5, a very good level of agreement is observed between the present ICS and those reported by Bettega *et al.*, within the uncertainties for the current data. As noted previously, in their SMC computations Bettega *et al.* did not include the Born-closure approach in their calculation of the dipole potential, so the computed ICS would likely increase a little in magnitude (the extent depending on the energy in question) if it was to be included [22]. This would result in the present measurements and the calculated ICSs being in even better accord than already seen in Fig. 5, particularly at the lower energies.

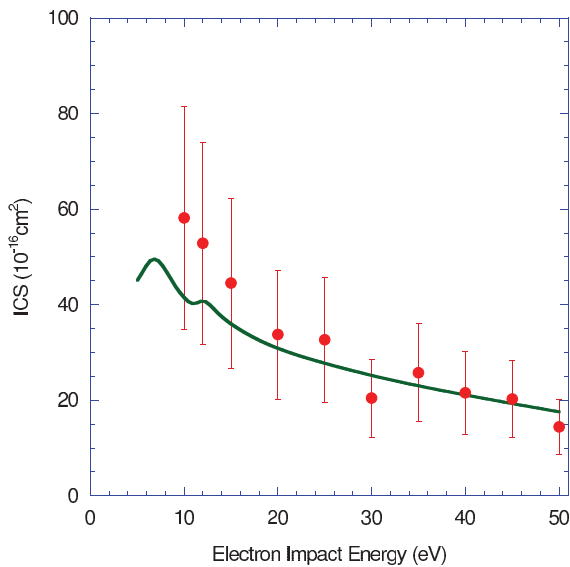


FIG. 5. (Color online) Elastic integral cross sections (10^{-16} cm^2) for electron impact on CF_3I from SMC calculations by Bettega *et al.* [11] (solid line) and the current measurements (\bullet).

IV. CONCLUSIONS

We have reported measurements of differential and integral elastic cross sections, for electron scattering off CF_3I , at ten incident electron energies in the range 10–50 eV. The present work significantly extends the available experimental data in this kinematic regime and, when combined with the lower energy results from Kitajima *et al.*, represents a comprehensive body of data against which the validity of scattering theories can be tested.

In general the present DCS results were found to be in very good agreement with the SMC calculations of Bettega *et al.* and the previous measurements of Kitajima *et al.*, except at the lowest energy of the current investigation. In addition, we highlight the excellent level of accord for the integral elastic cross sections, between Bettega *et al.* and our corresponding results, at all energies studied. We believe this indicates that the SMC computations can be reliably employed in models seeking to simulate the dynamics of plasma reactors, with

TABLE III. Experimental elastic integral cross sections (10^{-16} cm^2) of CF_3I for electron impact energies from 10 to 50 eV.

Energy (eV)	ICS ^a (10^{-16} cm^2)
10.00	58.20
12.00	52.90
15.00	44.55
20.00	33.78
25.00	32.68
30.00	20.46
35.00	25.77
40.00	21.59
45.00	20.27
50.00	14.43

^aUncertainties in the ICS measurements are on the order of 40%.

CF₃I as the feedstock gas. Finally, we note that the present elastic ICSs are also entirely consistent with the grand total-cross-section results from Kawada *et al.* [8].

ACKNOWLEDGMENTS

This work was supported by the Australian Research Council through its Centres of Excellence Program.

J.R.F.-S. acknowledges the Commonwealth of Australia for her Australian Postgraduate Award, while H.K. thanks the Japan Society for the Promotion of Science for his fellowships as grants-in-aid for scientific research and, most recently, to facilitate his visit to Flinders University and the Australian National University. We all thank Professor Marcio Bettega for sending tables of his computed results, and for helpful comments.

-
- [1] S. Raoux, M. B. T. Tanaka, H. Ponnekanti, M. Seamens, T. Deacon, L. Xia, F. Pham, D. Silveti, D. Cheung, and K. Fairbairn, *J. Vac. Sci. Technol. B* **17**, 477 (1999).
- [2] S. Solomon, J. B. Burkholder, A. R. Ravishankara, and R. R. Garcia, *J. Geophys. Res.* **99**, 20929 (1994).
- [3] I. Rozum, P. Limão-Vieira, S. Eden, J. Tennyson, and N. J. Mason, *J. Phys. Chem. Ref. Data* **35**, 267 (2006).
- [4] S. Samukawa and T. Mukai, *J. Vac. Sci. Technol. A* **17**, 2551 (1999).
- [5] T. Oster, O. Ingolfsson, M. Meinke, T. Jaffke, and E. Illenberger, *J. Chem. Phys.* **99**, 5141 (1993).
- [6] T. Makabe, *Adv. At. Mol. Opt. Phys.* **44**, 127 (2001).
- [7] L. G. Christophorou and J. K. Olthoff, *J. Phys. Chem. Ref. Data* **29**, 553 (2000).
- [8] M. K. Kawada, O. Sueoka, and M. Kimura, *Chem. Phys. Lett.* **330**, 34 (2000).
- [9] K. N. Joshipura, Minaxi Vinodkumar, C. G. Limbachiya, and B. K. Antony, *Phys. Rev. A* **69**, 022705 (2004).
- [10] M. Kitajima, M. Okamoto, K. Sunohara, H. Tanaka, H. Cho, S. Samukawa, S. Eden, and N. J. Mason, *J. Phys. B* **35**, 3257 (2002).
- [11] M. H. Bettega, A. P. P. Natalense, M. A. P. Lima, and L. G. Ferreira, *J. Phys. B* **36**, 1263 (2003).
- [12] C. Q. Jiao, G. Ganguly, C. A. De Joseph, and A. Garscadden, *Int. J. Mass Spectrom.* **208**, 127 (2001).
- [13] U. Onthong, H. Deutsch, K. Becker, S. Matt, M. Probst, and T. D. Märk, *Int. J. Mass Spectrom.* **214**, 53 (2002).
- [14] K. N. Joshipura, M. Vinodkumar, B. K. Antony, and N. J. Mason, *Eur. Phys. J. D* **23**, 81 (2003).
- [15] T. M. Maddern, L. R. Hargreaves, S. J. Buckman, and M. J. Brunger, *J. Phys. Conf. Ser.* **86**, 012005 (2007).
- [16] T. M. Maddern, L. R. Hargreaves, M. Bolorizadeh, M. J. Brunger, and S. J. Buckman, *Meas. Sci. Technol.* **19**, 085801 (2008).
- [17] T. M. Maddern, L. R. Hargreaves, J. R. Francis-Staite, and M. J. Brunger, *Meas. Sci. Technol.* **18**, 2783 (2007).
- [18] S. Götte, A. Gopalan, J. Bömmels, M.-W. Ruf, and H. Hotop, *Rev. Sci. Instrum.* **71**, 4070 (2000).
- [19] B. K. Antony, K. N. Joshipura, and N. J. Mason, *J. Phys. B* **38**, 189 (2005).
- [20] L. Boesten, H. Tanaka, A. Kobayashi, M. A. Dillon, and M. Kimura, *J. Phys. B* **25**, 1607 (1992).
- [21] K. M. Swift, L. A. Schlie, and R. D. Rathge, *Appl. Opt.* **27**, 4377 (1988).
- [22] M. H. F. Bettega (private communication).
- [23] C. S. Trevisan, A. E. Orel, and T. N. Rescigno, *Phys. Rev. A* **68**, 062707 (2003).
- [24] L. Campbell, M. J. Brunger, A. M. Nolan, L. J. Kelly, A. B. Wedding, J. Harrison, P. J. O. Teubner, D. C. Cartwright, and B. McLaughlin, *J. Phys. B* **34**, 1185 (2001).